



# Multivariate optimization on flow-injection electrochemical hydride generation atomic absorption spectrometry of cadmium

M.H. Arbab-Zavar<sup>a,\*</sup>, M. Chamsaz<sup>a</sup>, A. Youssefi<sup>b</sup>, M. Aliakbari<sup>a</sup>

<sup>a</sup> Department of Chemistry, Faculty of Sciences, Ferdowsi University of Mashhad, Mashhad, Iran

<sup>b</sup> Par-e-Tavous Research Institute, Mashhad, Iran

## ARTICLE INFO

### Article history:

Received 28 February 2012

Received in revised form

12 April 2012

Accepted 18 April 2012

Available online 10 May 2012

### Keywords:

Electrochemical hydride generation

Atomic absorption spectrometry

Flow-injection

Experimental design

Cadmium

## ABSTRACT

A novel electrochemical hydride generation (ECHG) system working in flow-injection (FI) mode was developed for determination of cadmium coupled to an electrically heated quartz tube atomizer (QTA) by atomic absorption spectrometry (AAS). A Plackett–Burman experimental design for screening has been used to evaluate the influence of several variables on the analytical response. Then, the significant parameters such as the concentration of NaCl in catholyte, applied electrolytic current and flow rate of carrier gas have been simultaneously optimized using a central composite design (CCD). Under the optimized conditions, the detection limit ( $3\sigma_b$ ,  $n=9$ ) was found to be  $0.51 \text{ ng mL}^{-1}$  Cd and the relative standard deviation (RSD) for nine replicate analyses of  $20 \text{ ng mL}^{-1}$  Cd was 6.5%. The calibration curve was linear in the range of  $2\text{--}50 \text{ ng mL}^{-1}$  of Cd. The potential interferences from various ions were also evaluated. The analysis of a reference material showed good agreement with the certified value. The proposed method was successfully applied to the determination of Cd in tap water sample.

© 2012 Elsevier B.V. All rights reserved.

## 1. Introduction

Chemical hydride generation (CHG), coupled with various atomic spectrometric detection techniques, has been commonly used for determination of classical hydride forming elements (HFEs) e.g. As, Bi, and Sb at trace levels [1–3]. Very recent publications indicate that similar to the well known CHG technique and cold vapor generation method for Hg [2] and Cd [4], the volatile species of an expanded range of elements including several transient and noble metals may be produced in the reduction reaction with sodium (or potassium) tetrahydroborate. The generation of volatile gaseous compounds of Au, Ag, Co, Cr, Cu, Fe, Ir, Mn, Ni, Pd, Pt, Rd, Ph, Os, Ti and Zn has been reported [5–7]. The characteristics and behavior of these species are not well known except that they are unstable and mostly molecular in nature [2,5,7].

For more than two decades, generation of cadmium volatile species by the reaction with  $\text{NaBH}_4$  has been an attractive alternative to the conventional sample introduction techniques owing to its enhanced detection power [4,8–11]. Feng et al. have reported that both atomic and molecular Cd species are generated in the reduction reaction, but a major fraction of gaseous products ( $\sim 95\%$ ) is atomic cadmium (cold vapor) [11].

Gaseous  $\text{CdH}_2$  molecules generated by the reactions of metal vapor with molecular hydrogen in the presence of an electrical

discharge and high-resolution infrared emission spectra of this molecule confirm its identity and the linear H–M–H structure [12,13]. The relative stability of this hydride supports the hypothesis that the molecule formed during the reduction of aqueous Cd ions in the CVG technique is  $\text{CdH}_2$  [7,12].

Electrochemical HG (ECHG) has been developed as a suitable alternative to chemical generation techniques [2,14,15]. The most significant advantage of the ECHG technique is the elimination of the use of  $\text{NaBH}_4$  reagent which is expensive, unstable and susceptible to contamination. Elemental Hg [16–18] and hydrides of As [16,19–22], Bi [16], Cd [23,24], Ge [16,22], Pb [25], Sb [16,19,21,22], Se [16,19–22], Sn [21–22], Te [26] and Tl [27] have been successfully generated by electrolytic method and these analytes were determined by a variety of atomic spectrometric techniques. Fundamental aspects and application of ECHG were discussed in two recent reviews [14,15]. The method probably involves the reaction of the deposited reduced analyte with the electrochemically generated hydrogen atoms on the cathode surface of the electrolytic cell.

Multivariate techniques are cost-effective, powerful and efficient statistical approaches, widely applied for optimization of analytical procedures. Compared with the traditional univariate methods, they provide several advantages such as the possibility of evaluating the effects of parameters and their mutual interactions by a reduced number of experiments [28,29].

In our earlier work [23], an ECHG system using semi-batch technique (B-ECHG), the cadmium hydride was generated and determined by AAS. It was found that the system produced sensitive and reproducible signals for trace amounts of cadmium.

\* Corresponding author. Tel: +98 511 8797022; fax: +98 511 8796416.

E-mail addresses: [arbab@um.ac.ir](mailto:arbab@um.ac.ir), [aliakbari.m@gmail.com](mailto:aliakbari.m@gmail.com) (M.H. Arbab-Zavar).

The generated cadmium hydride species were stable during their separation from the liquid phase and throughout the transportation processes to the detector. Nevertheless, the batch method suffers some disadvantages. The replacement of the cathode and sample after each determination was required. This was time-consuming and resulted in long analysis time. The sample throughput was  $10 \text{ h}^{-1}$ . The B-ECHG technique was also prone to interferences.

In this work, a flow-injection (FI) technique in combination with ECHG of Cd and on-line detection by atomic absorption spectrometry (AAS) preceded by atomization with electrically heated quartz tube (QTA) is described. The influences of several parameters on FI-ECHG of Cd were investigated using multivariate methods. Plackett–Burman design (PBD) for screening and central composite design (CCD) for optimization were carried out and optimum conditions were determined. The analytical figures of merit for the technique and its susceptibility to interference from various ions were evaluated and the developed method was applied to determine trace amount of cadmium in real samples.

## 2. Experimental

### 2.1. Instrumentation

A Shimadzu 680 atomic absorption spectrometer (Shimadzu, Japan) equipped with an electrically-heated quartz tube atomizer (QTA, 150 mm length, 4.2 mm i.d.) was used for atomic absorption measurements. Cadmium and lead hollow cathode lamps (Hamamatsu Photonics, Japan) operated at 4 and 7 mA and wavelengths of 228.8 and 217.0 nm, respectively were used as radiation sources both with 0.3 nm bandpasses. In-house software permitted the virtualization and evaluation of the transient signals.

### 2.2. Electrochemical hydride generation system

The home-made electrolytic flow-through cell was used to evaluate the electrochemical hydride generation (ECHG) of Cd. A schematic of the FI-ECHG-AAS system is shown in Fig. 1. The cell consists of cathodic and anodic compartments (both  $40 \times 6 \times 4 \text{ mm}^3$ , inner volumes of 1.0 mL) separated by a Nafion cation ion-exchange membrane (DuPont CO., USA). The four cell bodies, made of Plexiglas were held together tightly by four screws in order to prevent leakage and easy dismounting of the cell. Electrodes were mounted into appropriate chambers of the cell

through the electrode holders. This optimized design permitted easy replacement of the cathode with a new one. An injection valve (PIV1, Sabz Zist Kimiya Co., Iran) was used to inject the standards and samples. A Minipuls-3 peristaltic pump (Gilson, France) and a four-channel head were employed to transport the electrolytes and samples and withdrawing of the effluent. Some materials such as Pb and Sn bars, graphite rod, Pt wire and Pb–Sn wire were used as cathodes with a surface area of about  $1.0 \text{ cm}^2$ . Pb–Sn (Pb:Sn 37:63, diameter of 0.80 mm, Asahi, Singapore) was selected as the cathode material on the basis of the best preliminary results attained and also our early papers [23,24]. A coil of platinum (0.25 mm diameter,  $1.0 \text{ cm}^2$  surface area, Merck, Germany) was used as the anode. A programmable DC power source (Promax, FA-851, Promax Electronica S.A., Spain) was used as a constant current supply for the electrolytic cell. The carrier solution and the gaseous products from the cathode as well as the argon carrier gas stream controlled by a flow meter (Emerson Electronic co., USA) were transported into a laboratory-made gas–liquid separator (GLS, 10 mm i.d., 38 mm length). Consequently the generated volatile compounds were transferred through a 20-cm-long PVC tube (3.1 mm i.d.) to the atomizer, placed directly on the optical path of the atomic absorption spectrometer. The QTA was heated to a suitable temperature for atomization by applying a constant AC voltage. The connections were made by PVC tubing (2.05 mm i.d.).

### 2.3. Statistical treatment of data

Experimental design and statistical treatment of the results were performed using Minitab 16 software (Minitab Inc., USA).

### 2.4. Reagents and material

All reagents used in this work were of analytical grade (Merck, Germany). A standard stock solution of  $1000 \text{ mg L}^{-1}$  Cd was prepared by dissolving appropriate amounts of  $\text{CdCl}_2$  in ultrapure water. Working solutions were prepared by dilution of stock solution with dilute NaCl solution. Doubly-distilled water was used throughout. All solutions containing the potential interfering ions were prepared by adding appropriate amounts of stock solutions made from their corresponding salts (Table 5) in dilute NaCl ( $0.02 \text{ mol L}^{-1}$ ). Argon with 99.999% purity was used as the carrier gas.

### 2.5. Operating procedures

Electrochemical hydride generation performed in flow-injection mode was operated as follows: the blank carrier catholyte and anolyte solutions were continuously pumped into the cathode and anode chambers of the cell, respectively, at a flow rate of  $6.0 \text{ mL min}^{-1}$  by a peristaltic pump. The circulating anolyte ( $0.50 \text{ mol L}^{-1} \text{ Na}_2\text{CO}_3$ ) could be used for several days. At the same time, the cadmium sample was injected into the sampling loop of the injection valve at the same flow rate. If not stated otherwise, the standard sample was a solution of  $30 \text{ ng mL}^{-1}$  Cd in  $0.020 \text{ mol L}^{-1}$  NaCl and the carrier was pure  $0.020 \text{ mol L}^{-1}$  NaCl (blank catholyte). The electrolysis was started at a constant electrolytic current of 100 mA and carrier gas flow rate was set. Oxygen produced in the anode chamber was driven out along with the anolyte and then diffused into surroundings at the outlet of the transferring tube. The effluent was discharged from the GLS at a flow rate of  $8 \text{ mL min}^{-1}$ . After about 3–4 min of electrolysis time, injection of 1.0 mL sample into the catholyte carrier stream was performed manually via an injection valve and the sample was propelled to the cell. The sampling valve can be switched between the injection and loading positions every 30 s. The Ar gas

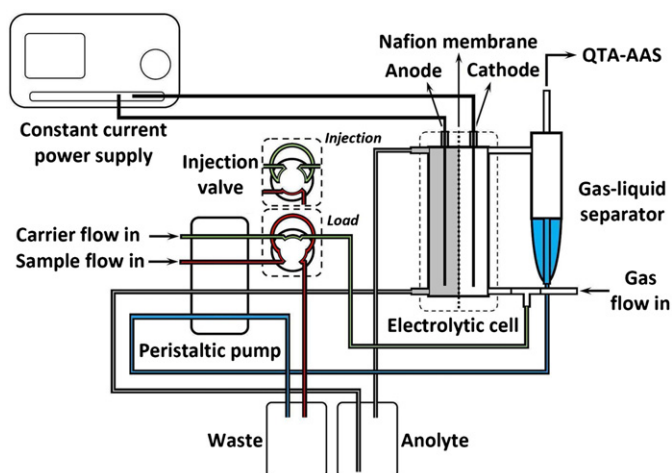


Fig. 1. Schematic diagram of the FI-ECHG-AAS system.

at a flow of  $100 \text{ mL min}^{-1}$  was introduced into the carrier stream before entering the input port of the electrochemical generator and has led the electrochemically generated products (Cd vapor and hydrogen) into the gas–liquid separator where the hydrides and the liquid were separated. The generated volatile species with excess hydrogen were directed by the argon carrier gas to the electrically-heated quartz tube atomizer adjusted at  $860 \pm 10 \text{ }^\circ\text{C}$  for the atomic absorption detection. The transient peak-shaped absorbance signals were recorded and the peak heights were used as the analytical responses. Improved sensitivity of Cd was observed when a neutral dilute solution was used as the catholyte. A complete cycle of the procedure lasted approximately 60 s. However because of the alteration of the cathode surface during electrolysis, the peak heights of the absorbance signals were slightly decreased, and therefore, the injections were repeated only for 10–15 min. The cathode was then easily exchanged and the whole procedure could be repeated. The analytical throughput of  $45 \text{ h}^{-1}$  was achieved.

### 3. Results and discussion

#### 3.1. Optimization of the experimental parameters

##### 3.1.1. Screening of significant factors using Plackett–Burman design

Large number of factors could potentially affect the FI–ECHG technique and therefore a Plackett–Burman (PB) design was used as a screening method to select the most statistically significant parameters for further optimization. The PB factorial design can identify main factors affecting the electrolytic hydride generation, separation and atomization processes by a relatively few experiments.

A Plackett–Burman type (III) resolution design for six factors, consisted of 12 non-randomized runs, was carried out. Evaluated factors were concentration of NaCl in catholyte ( $C_{\text{Cath}}$ ), applied electrolytic current ( $I$ ) and surface area of the cathode ( $A$ ) which are related to the electrolytic generation and flow rate of solutions ( $F_{\text{Soln}}$ ), argon carrier gas flow rate ( $F_{\text{Ar}}$ ) and atomization temperature ( $T$ ) relative to the separation and atomization processes. Based on the preliminary experiments, variations in the parameters considered might affect the analytical signal. The levels of the factors as low (–) and high (+), are listed in Table 1. These values were selected from the results of previous experiences and literature data [23]. Table 2 shows the PB experimental design matrix together with the analytical response (expressed as peak height) for each run.

The statistical evaluation of the results produced the standardized main effect Pareto chart as shown in Fig. 2 and offered a minimum  $t$ -value of 2.571 at a confidence level of 95.0%. In this chart bar lengths are proportional to the absolute values of the estimated effects and  $t$ -value is included as a vertical reference line. The variables which exceeded this reference line were considered as statistically significant factors. Furthermore, the positive and negative signs (corresponding to a grey and diagonal bar filling, respectively) showed that whether the response would be improved from the low to high level or not.

**Table 1**  
Experimental field definition for Plackett–Burman design.

Variable	Symbol	Low (–)	High (+)
Flow rate of solutions ( $\text{mL min}^{-1}$ )	$F_{\text{Soln}}$	3.0	6.0
Atomization temperature ( $^\circ\text{C}$ )	$T$	860	930
Concentration of NaCl in catholyte ( $\text{mol L}^{-1}$ )	$C_{\text{Cath}}$	0.010	0.020
Argon flow rate ( $\text{mL min}^{-1}$ )	$F_{\text{Ar}}$	80	100
Electrolytic current (mA)	$I$	75	100
Cathode surface area ( $\text{cm}^2$ )	$A$	1.0	1.2

**Table 2**  
Plackett–Burman experimental design matrix.

Run	$F_{\text{Soln}}$	$T$	$C_{\text{Cath}}$	$F_{\text{Ar}}$	$I$	$A$	Absorbance
1	+	–	+	–	–	–	0.1289
2	+	+	–	+	–	–	0.0795
3	–	+	+	–	+	–	0.1624
4	+	–	+	+	–	+	0.0904
5	+	+	–	+	+	–	0.1117
6	+	+	+	–	+	+	0.1672
7	–	+	+	+	–	+	0.1111
8	–	–	+	+	+	–	0.1060
9	–	–	–	+	+	+	0.0855
10	+	–	–	–	+	+	0.1212
11	–	+	–	–	–	+	0.1018
12	–	–	–	–	–	–	0.0826

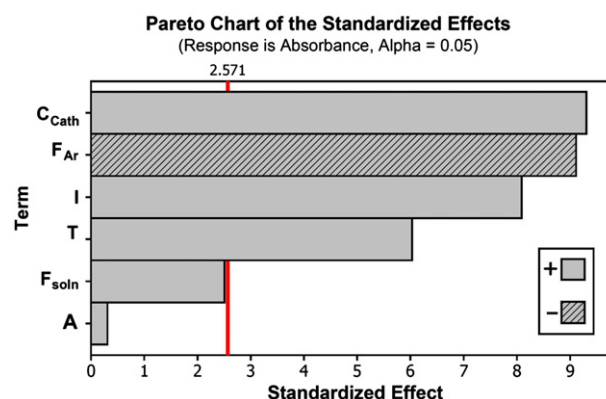


**Fig. 2.** Standardized main effect Pareto chart for Plackett–Burman design.

It can be seen that the following parameters, the concentration of NaCl, the applied current and the atomizer temperature are statistically significant and the effects of these variables are positive leading to enhanced analytical signals at their higher values. However, the flow rate of carrier gas is the next significant variable that is having a negative effect. Thus, the higher values of the sodium chloride concentration, the electrolytic current and the atomization temperature and lower carrier gas flow rate were selected for subsequent experiments. For the studied range of the parameters, the flow rate of catholyte and anolyte and the cathode surface area were not significant showing positive effects and, therefore, they were assigned at high level values for further experiments.

##### 3.1.2. Influence of atomization temperature

The atomizer temperature is one of the most important experimental parameters influencing the Cd signal intensity. The effect of the atomization temperature on the analytical absorbance signal was evaluated within an interval from room temperature to  $980 \text{ }^\circ\text{C}$ . The results indicated that no significant signal was observed below the temperature of  $300 \text{ }^\circ\text{C}$ . The absorbance of Cd rapidly increased with further increasing of the atomizer temperature and leveled off at temperatures in the range of  $930\text{--}980 \text{ }^\circ\text{C}$ . Therefore, an atomizer temperature of  $930 \text{ }^\circ\text{C}$  was selected for subsequent experiments to maintain the lifetime of the atomizer. The other significant parameters were chosen for further optimization by a central composite design (CCD).

##### 3.1.3. Optimization using central composite design

Based on the results of the screening design, a new optimization procedure was performed. Three variables including the NaCl

**Table 3**  
Experimental factors and their levels used in the central composite design (CCD).

Variable	Symbol	Axial ( $-\alpha$ )	Low ( $-1$ )	Center (0)	High (1)	Axial ( $\alpha$ )
Concentration of NaCl in catholyte ( $\text{mol L}^{-1}$ )	$C_{\text{Cath}}$	0.0116	0.0150	0.020	0.0250	0.0284
Electrolytic current (mA)	$I$	58	75	100	125	142
Argon flow rate ( $\text{mL min}^{-1}$ )	$F_{\text{Ar}}$	53	60	70	80	87

**Table 4**  
Central composite design matrix and the experimental results.

No.	Run	Coded values			Actual values			Absorbance
		$C_{\text{Cath}}$	$I$	$F_{\text{Ar}}$	$C_{\text{Cath}}$ ( $\text{mol L}^{-1}$ )	$I$ (mA)	$F_{\text{Ar}}$ ( $\text{mL min}^{-1}$ )	
1	16	-1	-1	-1	0.0150	75	60	0.1047
2	11	1	-1	-1	0.0250	75	60	0.1065
3	17	-1	1	-1	0.0150	125	60	0.0823
4	12	1	1	-1	0.0250	125	60	0.0576
5	18	-1	-1	1	0.0150	75	80	0.1363
6	13	1	-1	1	0.0250	75	80	0.1497
7	19	-1	1	1	0.0150	125	80	0.1167
8	14	1	1	1	0.0250	125	80	0.1063
9	20	$-\alpha$	0	0	0.0116	100	70	0.1084
10	15	$\alpha$	0	0	0.0284	100	70	0.1199
11	7	0	$-\alpha$	0	0.0200	58	70	0.1439
12	8	0	$\alpha$	0	0.0200	142	70	0.0987
13	9	0	0	$-\alpha$	0.0200	100	53	0.0601
14	10	0	0	$\alpha$	0.0200	100	87	0.1418
15	1	0	0	0	0.0200	100	70	0.1641
16	2	0	0	0	0.0200	100	70	0.1626
17	3	0	0	0	0.0200	100	70	0.1544
18	4	0	0	0	0.0200	100	70	0.1591
19	5	0	0	0	0.0200	100	70	0.1521
20	6	0	0	0	0.0200	100	70	0.1596

concentration of catholyte ( $C_{\text{Cath}}$ ), the working electrolytic current ( $I$ ) and the gas flow rate ( $F_{\text{Ar}}$ ) which all significantly influenced the analytical response were simultaneously optimized using a central composite design (CCD) and the effects as well as their mutual interactions were studied. This five-level fractional factorial design allows estimation of a second order (quadratic) model with linear, quadratic and interaction terms.

The CCD design with twenty experiments was carried out, consisting  $2^3$  full factorial design, augmented with  $2 \times 3$  axial (or star) points ( $\alpha=1.682$ ) and 6 replicates of the center point. Table 3 shows the selected factors and their domain i.e. low, central, high and axial levels. The complete design matrix and the corresponding analytical response of each run are presented in Table 4.

To find the most suitable fitting with the experimental data, a response surface model was developed using the regression analysis by considering different combinations of the linear, squared and interaction terms in polynomial equations. The adequacy of each model was checked using the analysis of variance (ANOVA) and a maximum  $p$ -value for lack-of-fit (LOF) of 0.254 ( $>0.05$ ) was obtained for the following equation suggesting that the quadratic model was significant. By applying the regression analysis, the following second-order polynomial equation was established to express a semi-empirical model for the electrolytic technique:

$$A_p = (-1.434) + 26.27 \times C_{\text{Cath}} + 4.737 \times 10^{-3} \times I + 2.996 \times 10^{-2} \times F_{\text{Ar}} + (-644.5) \times C_{\text{Cath}}^2 + (-2.174 \times 10^{-5}) \times I^2 + (-2.078 \times 10^{-4}) \times F_{\text{Ar}}^2 + (-0.05030) \times C_{\text{Cath}} \times I + 0.06475 \times C_{\text{Cath}} \times F_{\text{Ar}}$$

where  $A_p$  is the predicted absorbance values and  $C_{\text{Cath}}$ ,  $I$  and  $F_{\text{Ar}}$  are the actual values of the significant parameters.

The ANOVA test was performed to verify the statistical significance of the terms. The small resulted  $p$ -values ( $<0.05$ ) for the most of the squared and interaction terms, indicated their significance at 95% confidence level and suggested the presence of curvature in the response surface. However the interactions between the flow rate of argon carrier gas ( $F_{\text{Ar}}$ ) and the other parameters ( $C_{\text{Cath}} \times F_{\text{Ar}}$ ,  $p=0.147$  and  $I \times F_{\text{Ar}}$ ,  $p=0.626$ ) were found to be not significant. Neglecting the non-significant interaction term between the current ( $I$ ) and the flow rate of carrier gas ( $F_{\text{Ar}}$ ) led to improved fitting and increase the  $p$ -value for LOF from 0.208 to 0.254. The determination coefficient ( $R^2$ ) of 98.3% also confirmed that the model was well fitted to the experimental data.

The resulting two-dimensional (2D) contour plots for the pairs of parameters while the others kept constant at their middle values are illustrated in Fig. 3. They were used for determination of the optimum conditions and the interactions between the investigated factors. All shapes clearly show that the response surfaces are curved with a simple maximum in the domain of the experimental design. The signal improvement could be achieved with increasing the catholyte concentration ( $C_{\text{Cath}}$ ) up to an optimum value of  $0.021 \text{ mol L}^{-1}$  and then the response decreased. Similarly, it can be observed for both other parameters in Fig. 3, that the maximum response was achieved at an electrolytic current of 85 mA and argon flow rate of  $75 \text{ mL min}^{-1}$ .

The two-dimensional contour plots were also used for interpreting the mutual interaction between the factors. A response surface with an elliptical or saddle shape indicates a significant interaction between the corresponding variables, whereas a circular contour plot indicates negligible interaction [28–30]. The existence of interaction means that the factors may affect the response interactively and not independently. Therefore their combined effects are greater or less than that of expected for the addition of the particular effects. The inclined elliptical shape of the contour lines in Fig. 3a, also, confirmed that the interaction between  $C_{\text{Cath}}$  and  $I$  were significant. In contrast, the contour plots from the interactions between flow rate of argon carrier gas ( $F_{\text{Ar}}$ ) and other parameters (Fig. 3b and c) were approximately circular and so their interactions were insignificant.

In Fig. 3a, the absorbance signal is very low at high concentration of NaCl in carrier solution ( $C_{\text{Cath}}$ ) as the electrolytic current ( $I$ ) increases. In another experiment, the effects of  $C_{\text{Cath}}$  and  $I$  on the continuous generation of Pb hydride from the Pb–Sn cathode were studied within the experimental ranges. The recorded absorbance signals of Pb were found to increase with increasing the amounts of each one, suggesting that the instability of cathode surface may occur. However the applied electrolytic potential and consequently the overpotential decreased at high  $C_{\text{Cath}}$  values, presumably the conditions for the formation of the lead hydride molecules as well as the conductivity of the catholyte were improved by increasing the amount of NaCl. It can be concluded that the simultaneous increase of  $C_{\text{Cath}}$  and  $I$ , which resulted in cathode surface instability, decreased the electrochemical deposition of Cd and the hydride generation from the cathode surface.

### 3.2. Analytical figures of merit

Under the optimized experimental conditions, the analytical figures of merit for the procedure were determined. The calibration

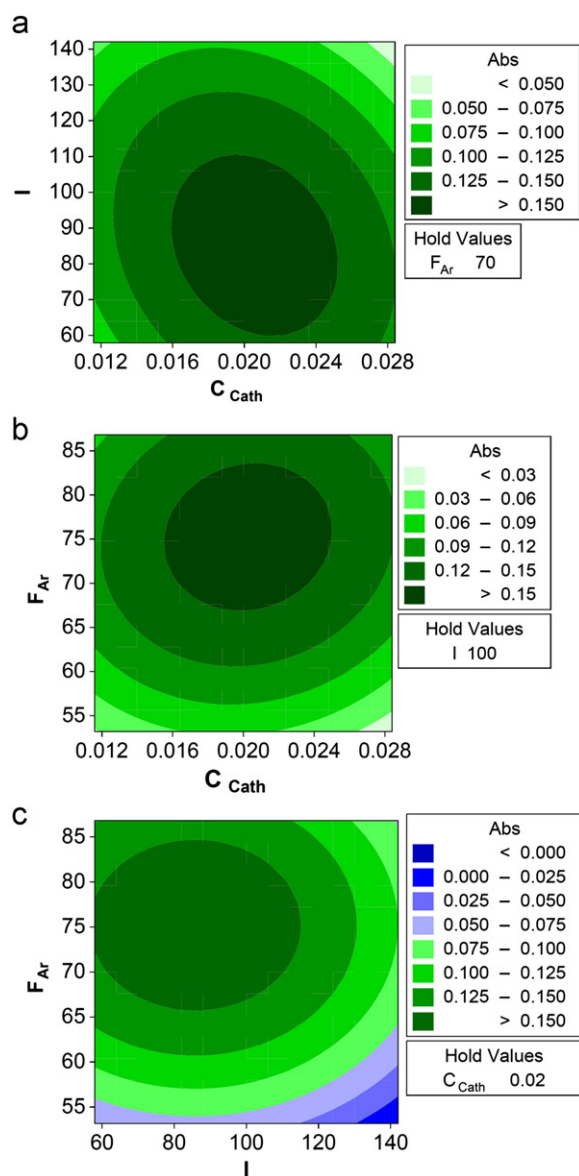


**Fig. 3.** Estimated contour (2D) plots from the central composite design for the analytical response as a function of (a)  $C_{\text{Cath}}$  and  $I$  ( $F_{\text{Ar}}$ : 70 mL min<sup>-1</sup>); (b)  $C_{\text{Cath}}$  and  $F_{\text{Ar}}$  ( $I$ : 100 mA) and (c)  $I$  and  $F_{\text{Ar}}$  ( $C_{\text{Cath}}$ : 0.020 mol L<sup>-1</sup>).

curve was linear in the range of 2–50 ng mL<sup>-1</sup> of cadmium. The calibration sensitivity and the concentration detection limit ( $3\sigma_b$ ,  $n=12$ ) were  $5.1 \times 10^{-3}$  (mL ng<sup>-1</sup>) and 0.51 ng mL<sup>-1</sup>, respectively. The repeatability precision (RSD) for nine replicate analyses at 20 ng mL<sup>-1</sup> of Cd was measured to be 6.5%.

### 3.3. Interferences

The interferences caused by a number of anions and cations in the determination of cadmium using FI-ECHG–AAS method were examined and expressed as the recovery relating to the signal obtained in the presence and absence of interferent ions. The analytical signal for standard solution of 20 ng mL<sup>-1</sup> Cd was measured in the presence of 2.0 or 20 mg L<sup>-1</sup> of the respective interfering ions. The results are shown in Table 5. Variations less than 10% of recovery may be considered insignificant. It was found that the presence of 20 mg L<sup>-1</sup> Ca<sup>2+</sup> and 2.0 mg L<sup>-1</sup> of Fe<sup>3+</sup>, Ni<sup>2+</sup>, Hg<sup>2+</sup> and Sn<sup>2+</sup> in the sample solution suppressed the response of Cd by 15%, 47%, 13%, 33% and 40%, respectively. Comparing with

**Table 5**

Interferences of various ions in determination of 20 ng mL<sup>-1</sup> Cd by FI-ECHG–AAS.

Species	Compound	Concentration (mg L <sup>-1</sup> )	Concentration ratio [M] <sup>a</sup> /[Cd]	Recovery (%mean ± S.D., $n=2$ )
NO <sub>3</sub> <sup>-</sup>	KNO <sub>3</sub>	20	1000	97 ± 4
SO <sub>4</sub> <sup>2-</sup>	Na <sub>2</sub> SO <sub>4</sub>	20	1000	93 ± 5
Mg <sup>2+</sup>	MgCl <sub>2</sub> · 6H <sub>2</sub> O	20	1000	95 ± 2
Ca <sup>2+</sup>	CaCl <sub>2</sub> · 2H <sub>2</sub> O	20	1000	85 ± 1
Fe <sup>3+</sup>	FeCl <sub>3</sub> · 6H <sub>2</sub> O	2.0	100	53 ± 10
Ni <sup>2+</sup>	NiCl <sub>2</sub>	2.0	100	87 ± 6
Cu <sup>2+</sup>	CuCl <sub>2</sub> · 2H <sub>2</sub> O	2.0	100	112 ± 7
Zn <sup>2+</sup>	ZnCl <sub>2</sub>	2.0	100	98 ± 3
Hg <sup>2+</sup>	HgCl <sub>2</sub>	2.0	100	67 ± 9
Sn <sup>2+</sup>	SnCl <sub>2</sub> · 2H <sub>2</sub> O	2.0	100	60 ± 8
Pb <sup>2+</sup>	Pb(NO <sub>3</sub> ) <sub>2</sub>	2.0	100	105 ± 3

<sup>a</sup> Interference ions.

previous ECHG technique for Cd [23], it was observed that employing the FI-ECHG decreased the interference effects of most cations and anions. The influence of the added metals can be explained by taking into account their electrodeposition on the cathode and the alteration of the surface chemistry and its hydrogen overpotential. Further studies are required to provide better understanding of the individual interfering effect and overcome the interferences. To eliminate any possible matrix effects in real samples, the technique of standard addition was used to obtain accurate results.

### 3.4. Analysis of a real sample

The proposed technique was applied to determine cadmium in real samples, a certified reference material (CRM), SRM 1643e (NIST) fresh water and a tap water sample. The tap water sample was collected from the city of Mashhad (NE Iran). The standard addition method was used to compensate the matrix effects on the ECHG of Cd. An appropriate volume of NaCl solution was added to the samples and they were diluted at a ratio of 1:2, yielding a resultant concentration of 0.021 mol L<sup>-1</sup> NaCl. To obtain spiked samples, another portion of the samples were spiked with the standard cadmium solution, supplemented with NaCl solution and diluted to the final added Cd concentration of 10.0 ng mL<sup>-1</sup>. The CRMs were neutralized with appropriate amounts of 2.0 mol L<sup>-1</sup> sodium hydroxide solution before dilution. The samples were analyzed under the optimum experimental conditions. The cadmium concentration of  $6.3 \pm 0.3$  ng mL<sup>-1</sup> was obtained in the CRM which is in acceptable agreement with the certified value of  $6.568 \pm 0.07$  ng mL<sup>-1</sup> (confidence interval of 95%). Using standard addition approach, the concentration of Cd in the tap water sample was determined to be  $2.3 \pm 0.3$  ng mL<sup>-1</sup>.

## 4. Conclusion

The FI-ECHG system was directly coupled to an electrically-heated quartz tube atomizer (QTA) atomic absorption spectrometry (AAS) and successfully applied to the determination of Cd in water samples. The molecular cadmium species, presumably CdH<sub>2</sub> molecules, were produced from the Pb–Sn cathode surface. Experimental designs such as PBD and CCD were applied to find a model for optimizing the technique. Although the achieved detection limit is slightly poorer than that observed with the previous batch method [23], the implementation of FI sample introduction provides additional advantages such as an increased sample throughput, reduced sample consumption, low cost, easy operation and reduced potential contamination. Furthermore, the need for the exchange of cathode after each measurement cycle was eliminated. It was shown that

interferences from major constituents were decreased using FI technique. It should be noted that the detection limit for the proposed method is not superior to the most of those reported in the literature using the chemical vapor generation of Cd [4,9,10,31] mostly because of the low efficiency of the FI-ECHG and instability of the vapor species. However, the developed system provides relatively easy, low cost and fast determination of Cd at trace levels. The enhancement of the performance and efficiency of the technique is ongoing. The system may be extended to the problematic hydride forming elements, e.g., In and Tl, and possibly other transition metals i.e. Zn and Ag. In fact, it was appeared from a preliminary examination of the FI-ECHG, that some elements such as Ag and Zn are amenable to this procedure.

## References

- [1] J. Dedina, D.L. Tsalev, *Hydride Generation Atomic Absorption Spectrometry*, John Wiley, New York, 1995.
- [2] R.E. Sturgeon, Z. Mester, *Appl. Spectrosc.* 56 (2002) 202A–213A.
- [3] P. Pohl, *Trends Anal. Chem.* 23 (2004) 21–27.
- [4] L. Lampugnani, C. Salvetti, D.L. Tsalev, *Talanta* 61 (2003) 683–698.
- [5] P. Pohl, B. Prusisz, *Anal. Bioanal. Chem.* 388 (2007) 753–762.
- [6] T. Matousek, *Anal. Bioanal. Chem.* 388 (2007) 763–767.
- [7] A. D'Ulivo, J. Dedina, Z. Mester, R.E. Sturgeon, Q. Wang, B. Welz, *Pure Appl. Chem.* 83 (2011) 1283–1340.
- [8] J. Cacho, I. Beltran, C. Nerin, *J. Anal. At. Spectrom.* 4 (1989) 661–663.
- [9] A. Sans-Medel, M.C. Valdes-Hevia y Temprano, N. Bordel Garcia, M.R. Fernandez de la Campa, *Anal. Chem.* 67 (1995) 2216–2223.
- [10] X.W. Guo, X.M. Guo, *J. Anal. At. Spectrom.* 10 (1995) 987–991.
- [11] Y.L. Feng, R.E. Sturgeon, J.W. Lam, *Anal. Chem.* 75 (2003) 635–640.
- [12] A. Shayesteh, S. Yu, P.F. Bernath, *Chem.: Eur. J.* 11 (2005) 4709–4712.
- [13] S. Yu, A. Shayesteh, P.F. Bernath, *J. Chem. Phys.* 122 (2005) 194301/1–194301/6.
- [14] E. Denkhaus, A. Golloch, X.-M. Guo, B. Huang, *J. Anal. At. Spectrom.* 16 (2001) 870–878.
- [15] F. Laborda, E. Bolea, J.R. Castillo, *Anal. Bioanal. Chem.* 388 (2007) 743–751.
- [16] N.H. Bings, Z. Stefanka, S.R. Mallada, *Anal. Chim. Acta* 479 (2003) 203–214.
- [17] X. Li, Z. Wang, *Anal. Chim. Acta* 588 (2007) 179–183.
- [18] V. Cervený, P. Rychlovský, J. Netolická, J. Sima, *Spectrochim. Acta B* 62 (2007) 317–323.
- [19] Y. Lin, X. Wang, D. Yuan, P. Yang, B. Huang, Z. Zhuang, *J. Anal. At. Spectrom.* 7 (1992) 287–291.
- [20] A. Brockmann, C. Nonn, A. Golloch, *J. Anal. At. Spectrom.* 8 (1993) 397–401.
- [21] E. Denkhaus, F. Beck, P. Bueschler, R. Gerhard, A. Golloch, *Fresenius J. Anal. Chem.* 370 (2001) 735–743.
- [22] E. Bolea, F. Laborda, J.R. Castillo, R.E. Sturgeon, *Spectrochim. Acta B* 59 (2004) 505–513.
- [23] M.H. Arbab-Zavar, M. Chamsaz, A. Youssefi, M. Aliakbari, *Anal. Chim. Acta* 546 (2005) 126–132.
- [24] M.H. Arbab-Zavar, M. Chamsaz, A. Youssefi, M. Aliakbari, *Anal. Chim. Acta* 576 (2006) 215–220.
- [25] M. Saenz, L. Fernandez, J. Dominguez, J. Alvarado, *Electroanalysis* 22 (2010) 2842–2847.
- [26] X. Jiang, W. Gan, S. Han, Y. He, *Spectrochim. Acta B* 63 (2008) 710–713.
- [27] M.H. Arbab-Zavar, M. Chamsaz, A. Yousefi, N. Ashraf, *Talanta* 79 (2009) 314–318.
- [28] S.L. Costa Ferreira, M. das Gracias Andrade Korn, H.S. Ferreira, E.G. Paranhos da Silva, R.G. Oliveira Araújo, A.S. Souza, S.M. Macedo, D. de Castro Lima, R.M. de Jesus, F.A. Carqueija Amorim, J.M. Bosque-Sendra, *Appl. Spectrosc. Rev.* 42 (2007) 475–491.
- [29] M.A. Bezerra, R.E. Santelli, E.P. Oliveira, L.S. Villar, L.A. Escalair, *Talanta* 76 (2008) 965–977.
- [30] R.V. Muralidhar, R.R. Chirumamila, R. Marchant, P. Nigam., *Biochem. Eng. J.* 9 (2001) 17–23.
- [31] W. Chuachud, J.F. Tyson, *J. Anal. At. Spectrom.* 20 (2005) 273–281.